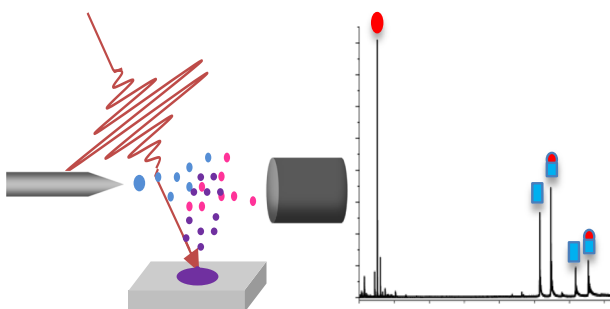**RESEARCH ARTICLE**

Quantification of Protein-Ligand Interactions by Laser Electrospray Mass Spectrometry

Jieutonne J. Archer, Santosh Karki, Fengjian Shi, Habiballah Sistani, Robert J. Levis

Department of Chemistry and Center for Advanced Photonics Research, Temple University, Philadelphia, PA 19122, USA

Abstract. Laser electrospray mass spectrometry (LEMS) measurement of the dissociation constant (K_d) for hen egg white lysozyme (HEWL) and N,N',N''-triacetylchitotriose (NAG_3) revealed an apparent K_d value of 313.2 ± 25.9 μM for the ligand titration method. Similar measurements for N,N',N'',N'''-tetraacetylchitotetraose (NAG_4) revealed an apparent K_d of 249.3 ± 13.6 μM. An electrospray ionization mass spectrometry (ESI-MS) experiment determined a K_d value of $9.8 \pm$ 0.6 μM. In a second LEMS approach, a calibrated measurement was used to determine a K_d value of $6.8 \pm$ 1.5 μM for NAG_3. The capture efficiency of LEMS was measured to be $3.6 \pm 1.8\%$ and is defined as the fraction of LEMS sample detected after merging with the ESI plume. When the dilution is factored into the ligand titration measurement, the adjusted K_d value was 11.3 μM for NAG_3 and 9.0 μM for NAG_4. The calibration method for measuring K_d developed in this study can be applied to solutions containing unknown analyte concentrations.

Keywords: Femtosecond, Laser, Electrospray ionization, Protein-ligand, Dissociation constant, Charge state distribution

Introduction

Electrospray ionization mass spectrometry (ESI-MS) investigations of non-covalent interactions provide information that can lead to the identification of binding partners and stoichiometry for protein-metal, protein-ligand, protein-protein, and protein-DNA complexes [1, 2]. Non-covalent interactions are usually quantified by measuring binding strength as represented by dissociation constant K_d for inhibitor screening and drug discovery [3–6]. In the most simple non-covalent protein-ligand system, apparent K_d is calculated by:

$$K_d = \frac{[P]_{eq}[L]_{eq}}{[PL]_{eq}} \tag{1}$$

where $[P]_{eq}$ is the concentration of free protein, $[L]_{eq}$ is the concentration of free ligand, and $[PL]_{eq}$ is the concentration of protein-ligand in solution equilibrium. When ESI-MS is used to determine K_d, the mass spectrometer is typically tuned to detect the peaks corresponding to the free protein and the protein-ligand complex, and the free ligand is not measured [2, 7–10]. In such measurements, the concentration of the protein is kept constant and the ligand is titrated into the ESI solution. A plot of $[PL]_{eq}/[P]_{eq}$ vs. $[L]_{eq}$ yields a straight line with its slope, m = $1/K_d$. The value for $[PL]_{eq}/[P]_{eq}$ is obtained directly from the mass spectra while $[L]_{eq}$ is calculated by subtracting the concentration of the protein-ligand complex from the initial ligand concentration [2, 9].

ESI-based techniques employed to study solution-based non-covalent molecular interactions have limitations [8, 11–13]. Desolvation during electrospray affects both intra- and inter-molecular electrostatic, H-bonding, and hydrophobic interactions [7]. One assumption is that the ion intensity of the observed complex and free molecule(s) represents an accurate measure of the relative solution phase concentrations [14–16]. Investigations have yielded binding strengths ranging from 6.0 $\pm$ 1.0 μM to 59.8 $\pm$ 17.6 μM for complexes of hen egg white

lysozyme (HEWL) and N,N',N''-triacetylchitotriose (NAG$_3$) [2, 8, 17, 18].

Laser-ESI hybrid techniques allow the decoupling of sampling and ionization steps [19]. Analyte sampling via desorption may occur by resonant matrix absorption of photon energy [20], thermal ablation [19, 21], or non-resonant multi-photon absorption [22]. ESI solution/solvents can be independently changed to control analyte ionization and charge distribution [23, 24]. Hybrid systems enable direct sampling of surfaces [19, 21, 22, 25, 26], enhanced quantitative analysis [19, 27], spatially resolved analysis [19, 28–32], and rapid throughput analysis [19]. Laser-assisted electrospray ionization (LAESI) has been used to analyze the interaction between human amylin and copper (II) ions for which an apparent K_d value was measured [33], that was an order of magnitude larger than that determined by fluorescence spectroscopy [34]. In the LAESI experiment, K_d values were calculated using the same titration method employed for ESI studies.

During the analysis of solution-based analytes by laser-ESI hybrid techniques, droplets generated by laser ejection are captured by charged droplets emerging from the ESI source [21, 22]. The union of these droplets causes a dilution of the original sample droplets followed by an increase in concentration as the solvent evaporates. The time lapse between the merging of the droplets and full desolvation is estimated to occur within a few milliseconds [24, 35]. This may be long enough for re-equilibration to occur between the non-covalent complex and free protein and ligand because the mechanical motions of lysozyme molecules required for substrate binding or release occurs within ~ 40 μs [36]. To measure accurate values for binding strengths using a laser-ESI hybrid technique, the concentration of the analytes within the droplets prior to desolvation should be considered.

Laser electrospray mass spectrometry (LEMS) is an ambient sampling technique that employs femtosecond, near-IR laser pulses to non-discriminately vaporized samples [22]. Unlike most other laser hybrid techniques, LEMS does not require sample preparation [19]. This attribute is important for investigating non-covalent protein-ligand interactions because sample preparation such as the addition of matrix molecules [20] or dehydration [21] typically denatures protein and reduces the ability to bind substrate. Hence, sample preparation may hamper the accurate measurement of binding strengths. Analytes investigated using LEMS acquire the same or less internal energy as those investigated using conventional ESI [37, 38]. LEMS has been used to successfully investigate lipids [39], proteins [22, 32, 40], and both wet and dry samples containing other biologically relevant analytes [19]. LEMS has been used to qualitatively investigate the non-covalent interactions between myoglobin and heme [23], and can yield quantitative analysis of surfaces [41] and mixtures [27] that is superior to conventional ESI. These studies suggest that the determination of non-covalent binding strengths using LEMS may be feasible.

We report here a new method by which LEMS can be used to quantitatively probe non-covalent interactions and binding strengths between the protein, hen egg white lysozyme (HEWL), and its ligand, N,N',N''-triacetylchitotriose (NAG$_3$). We measure an ESI calibration curve for NAG$_3$ in the presence of an internal standard to account for ESI intensity fluctuations and to determine the concentration of NAG$_3$ in the merged droplets. LEMS analysis was then performed on solutions containing a constant HEWL concentration and various concentrations of NAG$_3$. For comparison, we also investigated via separate LEMS and ESI titration methods using only protein measurements for calculation of K_d. The quantitative LEMS method reported here will allow K_d measurements to be made from samples of unknown concentrations. This has never been demonstrated by any other MS method. This method may be preferred to conventional ESI as it can also be applied for analysis of protein complexes directly from biological tissue surfaces, providing additional spatial information that would not be available if the sample is homogenized to perform conventional ESI measurements.

Experimental Section

Sample Preparation

Aqueous stock solutions of 5.0 mM NAG$_3$, 5.0 mM N,N',N'',N'''-tetracetylchitotetraose, NAG$_4$ (V-Labs Inc., Covington, LA, USA), 50.0 mM ammonium acetate (Sigma Aldrich, St. Louis, MO, USA), 4.0 mM 1,2-dihexanoyl-sn-glycero-3-phosphocholine DHPC (Avanti Polar Lipids, Inc., Alabaster, AL, USA), and 2.5 mM HEWL (Sigma Aldrich, St. Louis, MO, USA) were prepared in HPLC grade water (Fisher Scientific, Pittsburgh, PA, USA). All LEMS samples were prepared by combining and diluting stock solutions of HEWL and NAG$_3$ to create samples with a concentration of 250 μM HEWL and concentrations ranging from 0 to 500 μM NAG$_3$. The electrospray solvent used for K_d measurements by the LEMS ligand titration method was prepared by diluting the stock ammonium acetate solution with HPLC grade water to achieve a final concentration of 25 mM. The electrospray solvents used to calibrate the ligand intensity were prepared by combining and diluting stock solutions of ammonium acetate, DHPC, and NAG$_3$, to create electrospray solutions of 25.0 mM ammonium acetate, 400 nM DHPC, and concentrations ranging from 500 nM to 10 μM of NAG$_3$. The electrospray solvent used to measure K_d by the calibrated NAG$_3$ intensities contained 25.0 mM aqueous ammonium acetate and 400 nM DHPC. ESI ligand titration experiments were performed by combining and diluting stock solutions to create ESI samples of 10.0 μM HEWL and concentrations ranging from 2.0 to 10.0 μM NAG$_3$ with 25.0 mM ammonium acetate and 400 nM DHPC.

Laser Vaporization and Electrospray Ionization

The instrumentation for laser vaporization, electrospray ionization, and mass spectral detection has been previously described in detail [24]. A Ti:sapphire laser oscillator (KM

Laboratories, Boulder, CO, USA) seeded a regenerative amplifier (Coherent, Inc., Santa Clara, CA) to create a 2.5 mJ pulse centered at 800 nm with a duration of 70 fs, operating at 10 Hz to couple with the electrospray ion source. The laser was focused to a spot size of ~300 μM in diameter using a 16.9 cm focal length lens with an incident angle of 45° with respect to the sample. The intensity of the laser at the substrate was approximately 2×10^{13} W/cm^2. The steel sample plate was biased to -2.0 kV to compensate for the distortion of the electric field between the capillary and the needle caused by the sample stage. The area sampled was 6.4 mm below and 2 mm in front of the electrospray needle. The distance between the electrospray needle and the mass spectrometer inlet was 6.4 mm. Protein-ligand sample solutions were prepared by serial dilutions of stock solutions to achieve a final protein concentration of 250 μM while ligand concentration was varied from 0 to 250 μM. An aliquot of 6 μL sample solution was deposited unto a sample plate and then exposed to the focused laser beam until the entire sample was vaporized (~5 s). The sample was ejected in a direction perpendicular to the electrospray plume, where capture and ionization occurred.

The electrospray solution was pumped at a flow rate of 3 μL/min using a syringe pump (Harvard Apparatus, Holliston, MA, USA). The electrospray needle, with an internal diameter of 127 μM, was kept at ground. The MS inlet was biased to -4.5 kV. A countercurrent of nitrogen gas (180 °C) flowed at 4 L/min to assist the desolvation process. The vaporized and post-ionized analytes were analyzed by a high-resolution mass spectrometer (Bruker MicroTOF-Q II, Bruker Daltonics, Billerica, Germany) which was tuned for a wide m/z range (m/z between 200 and 2500). Prior to LEMS experiments, the mass spectrometer was calibrated with a solution of 99:1 (v/v) acetonitrile/ESI calibrant (#63606-10 ML, Fluka Analytical/Sigma Aldrich, Buchs, Switzerland) over a mass range of m/z 50-3000. Raw spectra were recorded at a rate of 1 Hz and then averaged, processed, and analyzed using Compass Data Analysis 4.0 Software by Bruker Daltonics.

Results and Discussion

Determining K_d Values via LEMS Ligand Titration

To perform the LEMS measurement of K_d for the HEWL-NAG$_3$ complex, an aqueous solution containing 250 μM of HEWL was first laser vaporized into an ESI plume containing 25 mM ammonium acetate. The LEMS spectrum contained two dominant ion features at m/z 1789.1 and 2044.6 which correspond to $[M + 8H]^{8+}$ and $[M + 7H]^{7+}$, respectively (Figure 1a) suggesting that the HEWL is in the native, folded conformation in the droplets. [42] Two minor ion features were also detected at m/z 1590.4 and 2385.1 which correspond to $[M + 9H]^{9+}$ and $[M + 6H]^{6+}$, respectively (Figure 1a) LEMS of HEWL revealed a deconvoluted molar mass of ~14,304.8 amu which is in agreement with the molar mass of 14,304.7 amu obtained from an ESI experiment and the theoretical molar mass of HEWL of ~14,305.1 amu [2]. A 6 μL aliquot of
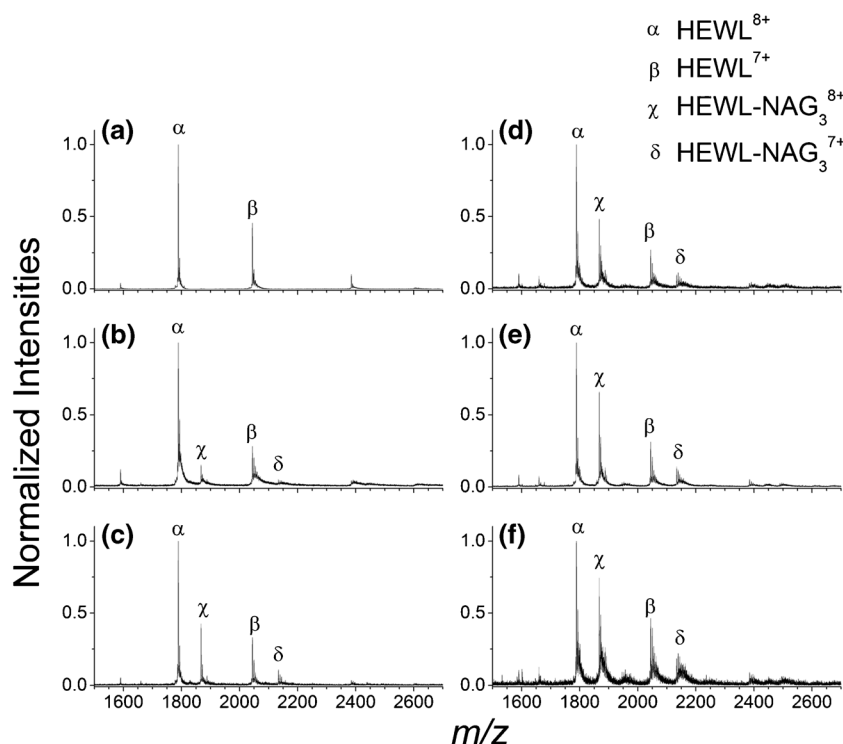

Figure 1. Mass spectra representing laser-induced vaporization of 250 μM HEWL with (a) 0 μM, (b) 50 μM, (c) 100 μM, (d) 150 μM, (e) 200 μM, (f) 250 μM NAG$_3$ into the ES of 25 mM aqueous ammonium acetate. The m/z range is extended to include minor ion features at m/z 1590.4 and 2385.1 which correspond to HEWL $[M + 9H]^{9+}$ and $[M + 6H]^{6+}$ respectively. Minor ion signals at m/z 1660.2 and 2489.8 correspond to the HEWL-NAG$_3$ complex $[M + 9H]^{9+}$ and $[M + 6H]^{6+}$ charge states, respectively

250 μM HEWL sample solution containing 0 to 250 μM NAG$_3$ was deposited onto the sample stage and laser vaporized into an aqueous ESI plume containing 25 mM ammonium acetate. LEMS analysis of a solution of HEWL and NAG$_3$ revealed three major additional ion signals (Figure 1b–f). The peaks at m/z 1867.6 and 2134.3 correspond to the HEWL-NAG$_3$ complex $[M + 8H]^{8+}$ and $[M + 7H]^{7+}$ charge states, respectively (see Figure 1), and a peak at m/z 628.3 (not shown) that corresponds to free NAG$_3$. Two additional minor ion signals at m/z 1660.2 and 2489.8 corresponds to the HEWL-NAG$_3$ complex $[M + 9H]^{9+}$ and $[M + 6H]^{6+}$ charge states, respectively (Figure 1b–f) These LEMS measurements reveal that the deconvoluted molar mass of the complex between HEWL and NAG$_3$ is 14,932.8 amu. The difference in the measured mass between HEWL and HEWL-NAG$_3$ complex is 628.0 amu which is in agreement with the molar mass of NAG$_3$ (627.6 amu).

The abundance ratio (R) of all detected charge states, for free HEWL and HEWL-NAG$_3$ complex, was assumed to represent the ratio of HEWL-NAG$_3$ complex and free HEWL concentrations in solution using

$$\frac{[PL]_{eq}}{[P]_{eq}} = \frac{\sum I \, [P{\cdot}L]^{n+}}{\sum I \, [P]^{n+}} = R \qquad (2)$$

where $\sum I \, [P{\cdot}L]^{n+}$ represents the sum of the signal intensity corresponding to HEWL-NAG$_3$ complex and $\sum I \, [P]^{n+}$ represents the sum of the signal intensity corresponding to free HEWL. The value of K$_d$ was determined by constructing a plot of R vs. free NAG$_3$ (Eq. 3) [2, 9]:

$$\frac{1}{K_d} = \frac{R}{[L]_i - \dfrac{R[P]_i}{R+1}} \qquad (3)$$

where $[L]_i$ is the initial concentration of NAG$_3$ and $[P]_i$ is the initial concentration of HEWL and the denominator on the right side represents the concentration of free NAG$_3$. In this approach, the MS peak intensity of free NAG$_3$ is not considered, instead the denominator in Eq. 3 is used to calculate the concentration of free NAG$_3$. Inspection of Figure 1b–f reveals that the ion intensities for the complex at m/z 1867.6 and 2134.3 increases as the total NAG$_3$ concentration increases. The R value was plotted as a function of the concentration of free ligand in Figure 2 and the inverse of the slope of the best-fit line (m^{-1}) represents K$_d$. In the construction of the best-fit line, each point was weighted based on the inverse square of the error bars. The apparent K$_d$ value for HEWL-NAG$_3$ complex was 313.2 ± 25.9 μM (Table 1). This value is almost two times larger than the K$_d$ value of 169.1 μM measured by reactive desorption electrospray ionization mass spectrometry (DESI-MS). In the reactive DESI experiment, the mixing of HEWL and NAG$_3$ occurred after the Taylor cone and the large K$_d$ value was attributed due to poor mixing within the droplets [46]. A K$_d$ value of 11.1 μM was measured by isothermal
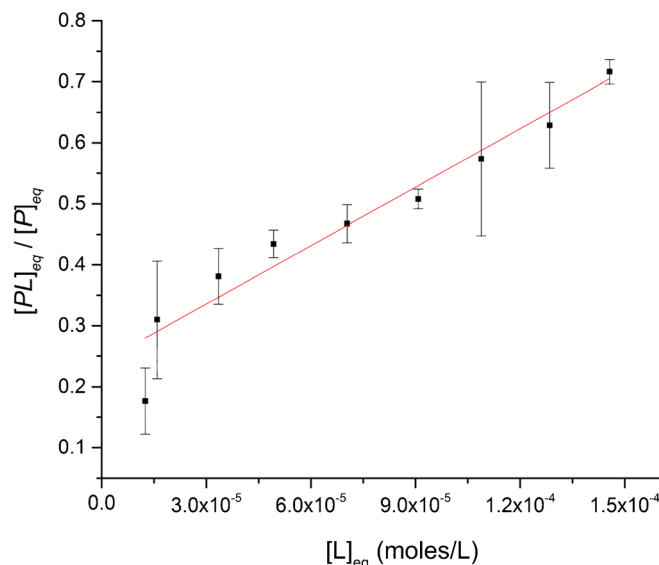

Figure 2. LEMS titration plot of HEWL-NAG$_3$/free HEWL concentration as a function of the free NAG$_3$ concentration calculated using the denominator in Eq. 3. The value of the slope's inverse gives a K$_d$ value of 313.2 ± 25.9 μM ($R^2 = 0.93$). Error bars correspond to ± 1 standard deviation of three measurements

titration calorimetry (ITC), which is considered the standard for quantifying protein-carbohydrate interactions [45].

The K$_d$ value of the HEWL-NAG$_4$ complex was determined to further test the method. LEMS spectra of HEWL and NAG$_4$ are shown in supplementary Fig. S1. Ion signals corresponding to free HEWL and HEWL-NAG$_4$ complex were detected for charge states ranging from 9+ to 6+. From these measurements, a titration plot was constructed as shown in supplementary Fig. S2 and the inverse of the slope revealed an apparent K$_d$ value of 249.3 ± 13.6 μM for HEWL-NAG$_4$ complex. As in the NAG$_3$ experiment, the apparent value for the K$_d$

Table 1. Literature and Experimental K$_d$ Values for lysozyme-NAG$_3$ Calculated by Different Methods

Method	Kd (μM)
Diffusion MS [17]	6.0 ± 1.0
UV [43]	6.6
LEMS[a]	6.8 ± 1.5
Fluorescence [44]	8.6
ESI [42]	9.24 ± 0.58
ESI[b]	9.8 ± 0.6
ESI [2]	10.0
DESI [45]	10.0
ITC [45]	11.1
LEMS[c]	11.3
ESSI [8]	19.4 ± 3.6
NanoESI [8]	39.8 ± 8.1
ESI [8]	59.8 ± 17.6
Reactive DESI [46]	169.1
LEMS[d]	313.2 ± 25.9

[a]K$_d$ value calculated via LEMS ligand intensity calibration method
[b]K$_d$ value calculated via ESI ligand titration method (current experiment)
[c]K$_d$ value calculated via adjusting value of LEMS ligand titration method
[d]K$_d$ value calculated via LEMS ligand titration method

of HEWL-NAG$_4$ complex is more than an order of magnitude larger than the K$_d$ value of 9.1 μM measured by isothermal titration calorimetry (ITC) [45]. The apparent K$_d$ for NAG$_4$ is less than that for NAG$_3$ and is consistent with the decrease in K$_d$ from NAG$_3$ to NAG$_4$ that has been previously reported [2, 45].

Determining K$_d$ Values via ESI Ligand Titration

As a comparison to the apparent K$_d$ value measured via the LEMS titration experiment, an ESI titration experiment was carried out to measure the K$_d$ value of the HEWL-NAG$_3$ complex. ESI solutions of 25.0 mM ammonium acetate, 400 nM 1,2-dihexanoyl-sn-glycero-3-phosphocholine (DHPC) used as an internal standard, 10.0 μM HEWL, and concentrations ranging from 2.0 μM to 10.0 μM of NAG$_3$ were prepared and analyzed. A shift to higher charge states was observed with increasing ligand concentration with saturation in the shift occurring at approximately 8.0 μM (Figure 3). A shift in charge state distribution was not observed in the LEMS measurements which were taken at concentrations that were an order of magnitude higher than the ESI measurements (Figure 1). This shift in charge state coincides with a previously reported change in the conformation of lysozyme in the presence of a substrate [36]. Charge states corresponding to $[M + 6H]^{6+}$, $[M + 7H]^{7+}$, $[M + 8H]^{8+}$, and $[M + 9H]^{9+}$ were used in Eqs. 2 and 3. To

determine K$_d$, the R value was plotted as a function of the concentration of free ligand in Figure 4. In the construction of the best-fit line, each point was weighted based on the inverse square of the error bars. The K$_d$ value for HEWL-NAG$_3$ complex was 9.8 ± 0.6 μM which is in agreement with the K$_d$ value of 11.1 μM measured by ITC [45]. This suggests that the large apparent K$_d$ value measured in the LEMS experiment is not due to dissociation of the complex in the gas phase.

Two plots were constructed to analyze the system response between the measured ion signal intensity of free NAG$_3$ and the calculated concentration of free NAG$_3$ based on the denominator of Eq. 3. A plot of the measured ion signal intensity of NAG$_3$ (*m/z* 628.3) as a function of the calculated concentration of free NAG$_3$ revealed poor linearity, with an R^2 value of 0.50 as shown in supplementary Fig. S4. Conversely, a plot of the ion signal intensity of NAG$_3$ divided by the ion signal intensity of the internal standard DHPC (*m/z* 454.3) as a function of the calculated concentration of free NAG$_3$ revealed better linearity with an R^2 value of 0.79 as shown in Figure 5.

Determining K$_d$ Values via Ligand Intensity Calibration

A calibration curve for the ESI response of NAG$_3$ was measured to determine the concentration of free ligand in the

α HEWL^{8+}
β HEWL^{7+}
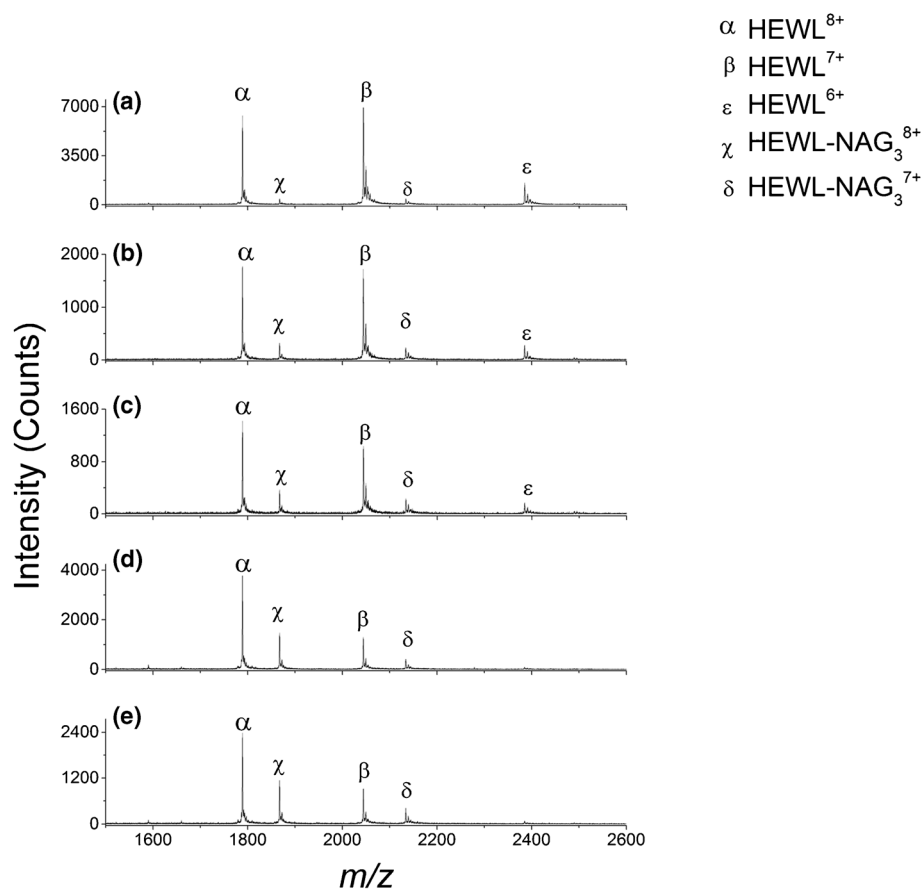ε HEWL^{6+}
χ HEWL-NAG$_3$$^{8+}$
δ HEWL-NAG$_3$$^{7+}$

Figure 3. Mass spectra representing ESI-MS of 25 mM aqueous ammonium acetate, 400 nM DHPC, and 10 μM HEWL with (a) 2 μM, (b) 4 μM, (C) 6 μM, (d) 8 μM, (e) 10 μM NAG$_3$
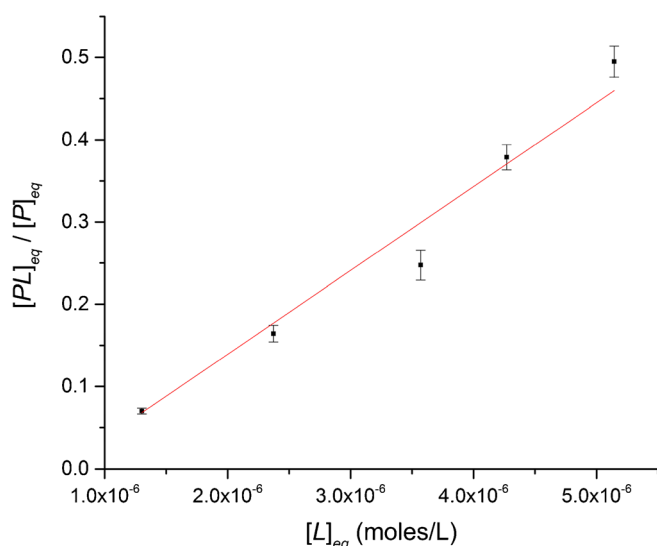
Figure 4. ESI titration plot of HEWL-NAG$_3$/free HEWL concentration as a function of the free NAG$_3$ concentration calculated using the denominator in Eq. 3. The value of the slope's inverse gives a K$_d$ value of 9.8 ± 0.6 μM (R^2 = 0.98). Error bars correspond to ± 1 standard deviation of three measurements

droplet after laser vaporization. The concentration of free ligand can then be used to further refine K$_d$. ESI solutions were prepared with concentrations of NAG$_3$ varying between 500 nM and 10 μM. The lipid 1,2-dihexanoyl-sn-glycero-3-phosphocholine (DHPC) was used as an internal standard at a concentration of 400 nM in 25 mM ammonium acetate to normalize for variation in the ESI signal intensities. The
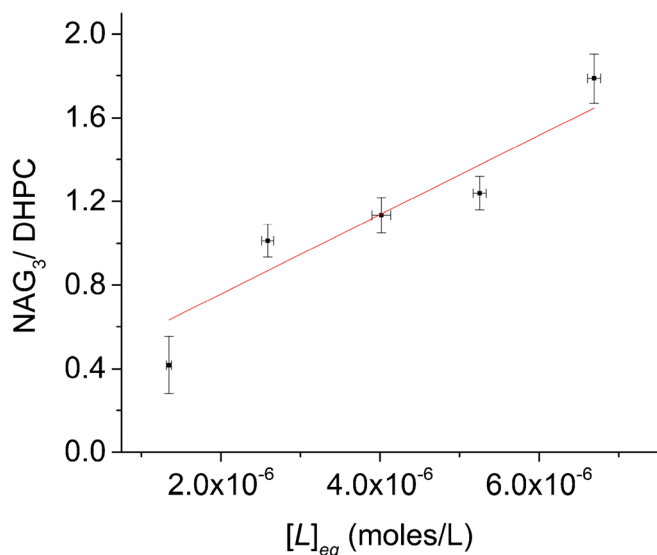

Figure 5. ESI titration plot for the ion signal intensity of NAG$_3$ divided by the ion signal intensity of DHPC as a function of free NAG$_3$ concentration calculated using the denominator in Eq. 3. Resulting data points correspond to aqueous NAG$_3$ concentrations of 2.0 μM, 4.0 μM, 6.0 μM, 8.0 μM, and 10.0 μM, respectively, with 10 μM of HEWL, 400 nM DHPC, and 25 mM ammonium acetate. R^2 = 0.79 and error bars correspond to ± 1 standard deviation of three measurements

relative intensity ratio of NAG$_3$ and internal standard was plotted as a function of the concentration of NAG$_3$ to produce the calibration curve. The resulting spectra show a linear increase in the intensity of the NAG$_3$ ion at m/z 628.3 relative to the DHPC ion at m/z 454.3 as the NAG$_3$ concentration is increased (Figure 6). A plot of the intensity of NAG$_3$ (m/z 628.3) divided by the intensity DHPC (m/z 454.3) as a function of the known concentration of NAG$_3$ reveals an R^2 value of 0.99, as shown in Figure 7. For comparison, a plot of the ion intensity of NAG$_3$ as a function of concentration without consideration of the internal standard reveals an R^2 value of 0.15 as shown in supplementary Fig. S3, presumably due to variation in the ESI system. An internal standard was not considered for calibrating the absolute signal intensities of HEWL and HEWL-NAG$_3$ complex because the ratio of the relative intensities of the mass spectral responses observed for both species reflects the ratio of HEWL to HEWL-NAG$_3$ complexes assuming the instrument response function is the same for each species.

The concentration of free ligand captured within the ESI plume, $[L]_{capt}$, during the analysis of HEWL-NAG$_3$ solutions was determined by Eq. 4, which was obtained from the best-fit line of the NAG$_3$ calibration curve in Figure 7.

$$[L]_{capt} = \frac{\left(\frac{(I)NAG_3}{(I)DHPC}\right) + 0.034}{128114\left(\frac{L}{mol}\right)} \quad (4)$$

where $(I)NAG_3$ represents the intensity of NAG$_3$ and $(I)DHPC$ represents the intensity of DHPC (internal standard), 0.034 is the value of the y-intercept of Figure 7 and 128,114 L/mol is the slope of the data in Figure 7.

LEMS analysis was performed on 6 μL aliquots of aqueous solutions containing 250 μM lysozyme with concentrations varying from 100 to 500 μM NAG$_3$. Samples were laser vaporized into an aqueous electrospray solution containing 400 nM of the internal standard and 25 mM ammonium acetate. The resulting spectra contained features corresponding to DHPC, NAG$_3$, the 7+, 8+, and 9+ charge states of HEWL, and the corresponding charge states of HEWL-NAG$_3$ complex (Figure 8). The ratio between the detected free NAG$_3$ and internal standard intensities was used to determine the concentration of free NAG$_3$ within the ESI droplet, $[L]_{capt}$. The K$_d$ values were then determined using $[L]_{capt}$ and the ratio of the intensities of HEWL-NAG$_3$ complex and free HEWL (Eq. 5).

$$K_d = \frac{[L]_{capt}[P]_{eq}}{[PL]_{eq}} = \frac{[L]_{capt}}{R} \quad (5)$$

Three measurements were made for each concentration and the averages of these values were then used to determine K$_d$. The K$_d$ values ranged from 5.1 to 8.4 μM (Table 2). These results are in agreement with other studies as seen in Table 1. The much higher K$_d$ value measured by LEMS without $[L]_{capt}$
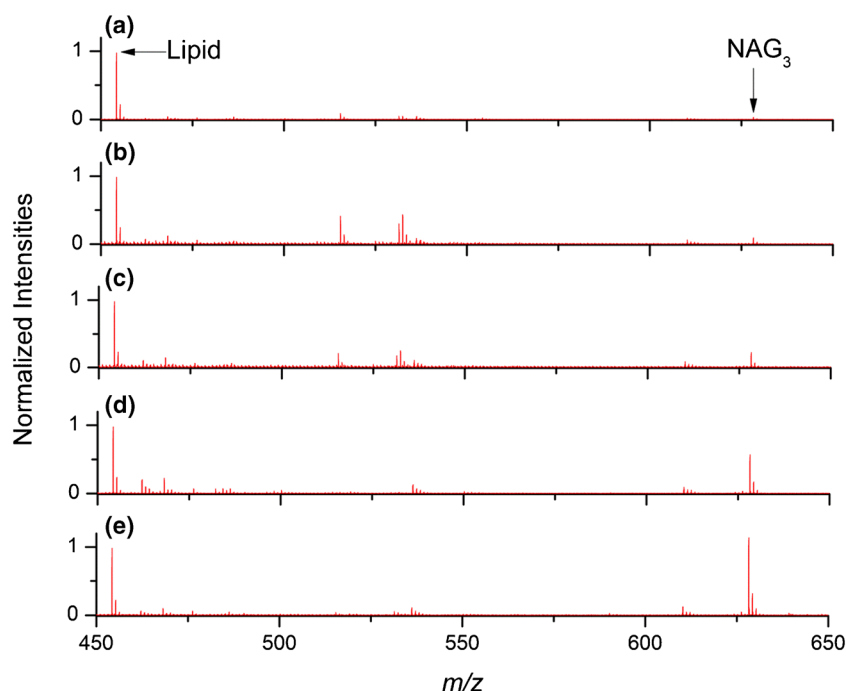
Figure 6. Representative ESI mass spectra of 400 nM DHPC as an internal standard with (a) 500 nM, (b) 1 μM, (c) 2 μM, (d) 5 μM, (e) 10 μM of NAG$_3$. All unlabeled peaks are ESI solvent background ions

suggests that there is a re-equilibrium between the HEWL and NAG$_3$ after merging of the laser-vaporized droplets with the electrospray-generated droplets.

The calibration method provides a means to calculate a precise capture efficiency of LEMS from the amount of sample detected in the mass spectrometer. After laser vaporization into an ESI plume, the analyte concentration may be less than that in the original sample due to the additional electrospray droplet volume. The concentration then decreases because the vaporized analyte droplets merge into the droplets from the ESI

plume, increasing the total volume. To determine the extent of the effective dilution of the analyte, we assumed that droplets generated from the vaporization of solution maintain the original molar ratio of all initial species. This can be represented by the following expression:

$$\frac{[L]_i}{[P]_i} = \frac{[L]_{drop}}{[P]_{drop}} \cdot [L]_{drop} = \frac{[L]_i \cdot [P]_{drop}}{[P]_i} \quad (6)$$
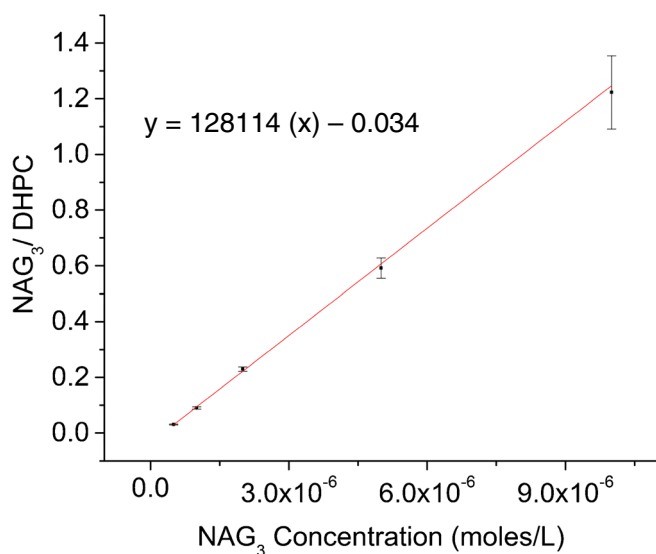

Figure 7. Calibration curve for the ESI response of NAG$_3$ with 400 nM DHPC as an internal standard ($R^2 = 0.99$). The error bars correspond to ± 1 standard deviation of three measurements
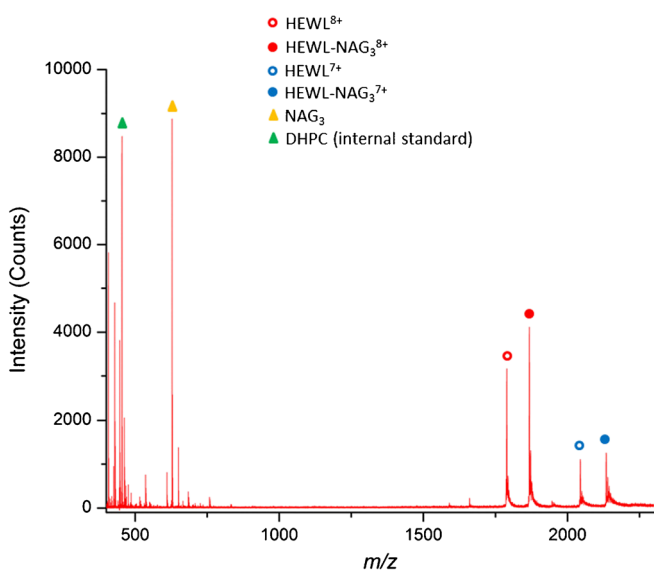

Figure 8. Mass spectra representing laser-induced vaporization of 400 μM NAG$_3$ and 250 μM HEWL into the ES plume containing 25 mM aqueous ammonium acetate with 400 nM DHPC

Table 2. The Individual K_d Values for Lysozyme-NAG$_3$ Calculated via LEMS Measurements for Various Concentrations using the Ligand Intensity Calibration Method

NAG$_3$/Lyz (µM)	K_d (µM)
100/250	5.6
200/250	5.1
300/250	8.4
400/250	6.9
500/250	8.1
Average K_d	6.8
Std. Dev.	1.5

where $[L]_{drop}$ represents the total concentration of ligand captured in the ESI plume, $[L]_i$ represents the initial ligand concentration in the LEMS sample, $[P]_{drop}$ represents the total concentration of protein captured in the ESI plume, and $[P]_i$ represents the initial protein concentration in the LEMS sample. K_d can be represented by the following equation using the droplet concentrations, $[L]_{drop}$ and $[P]_{drop}$.

$$\frac{1}{K_d} = \frac{R}{[L]_{drop} - \dfrac{R\,[P]_{drop}}{R+1}} \tag{7}$$

We can solve for the value of $[P]_{drop}$ by substituting the expression for $[L]_{drop}$ in Eq. (6) into Eq. (7) to yield the following.

$$K_d R = [P]_{drop}\left(\frac{[L]_i}{[P]_i} - \frac{R}{R+1}\right) \tag{8}$$

The individual K_d value corresponding to each concentration (Table 2) was used to solve $[P]_{drop}$. The initial concentration of protein $[P]_i$ in all LEMS samples was 250 µM and our calculations yielded an average $[P]_{drop} = 8.9$ µM which suggests that the capture efficiency of LEMS is $3.6 \pm 1.8\%$. This value is in agreement with the capture efficiency of $2.4 \pm 1.5\%$ reported for oxycodone on steel sample plates using LEMS [47]. A K_d value adjusted for the dilution factor can be calculated by assuming that 3.6% of the LEMS sample concentration is captured into the ESI plume. The adjusted concentration of free ligand is calculated by:

$$[L]_{adj} = 0.036\left([L]_i - \frac{R[P]_i}{R-1}\right) \tag{9}$$

where $[L]_{adj}$ is the value of the free ligand within the droplet assuming that 3.6% of the LEMS sample is captured. Using the dilution factor as similarly reported in a reactive DESI experiment [46], the original HEWL-NAG$_3$ K_d value of 313.2 µM becomes 11.3 µM which is in agreement with values reported in literature (Table 1). The same dilution factor was used for HEWL-NAG$_4$, providing a K_d value of 9.0 µM which is in agreement to the value of 9.1 µM reported for ITC measurements [45].

Conclusions

We have used LEMS to study the non-covalent protein-ligand interaction between lysozyme and NAG$_3$. We have used two different methods to solve for the K_d values. The first method used the ligand titration scheme that is generally used for ESI studies. This method yielded an apparent K_d value of 313.2 ± 25.9 µM which is more than an order of magnitude larger than the K_d values obtained via other conventional ESI-MS methods. An ESI ligand titration experiment was used to measure K_d value of 9.8 ± 0.6 µM. This suggests that in the LEMS experiment, dissociation of the complex is not occurring in the gas phase. We hypothesize that the apparent high K_d value measured with LEMS is because the capture efficiency and ESI droplet volume decreases the concentration of ligand and protein in the ESI droplets. Assuming the complex re-equilibrates, the decrease in concentration would increase the apparent K_d value. The second LEMS method accounts for the ligand concentration using an ESI calibration curve measured with an internal standard prior to LEMS analysis of protein-ligand solutions. The intensity of the free ligand relative to the internal standard was used to calculate the effective concentration of the ligand after the laser-vaporized sample was captured by electrospray droplets. The effective ligand concentration was then used along with protein and protein-ligand complex MS signals to determine a K_d value of 6.8 ± 1.5 µM which is in agreement to other reported values. The calibration method can be used to probe solutions containing unknown analyte concentrations. The calibration also allowed the calculation of the capture efficiency of LEMS. The measurement suggested that ~3.6% of the original sample concentration is captured in the ESI plume. When this is factored into the original LEMS ligand titration experiments, the adjusted K_d values for NAG$_3$ and NAG$_4$ are 11.3 and 9.0 µM respectively. These values are also in agreement with previously reported ITC K_d measurements [45].

References

1. Veenstra, T.D.: Electrospray ionization mass spectrometry in the study of biomolecular non-covalent interactions. Biophys. Chem. **79**, 63–79 (1999)
2. Veros, C.T., Oldham, N.J.: Quantitative determination of lysozyme-ligand binding in the solution and gas phases by electrospray ionisation mass spectrometry. Rapid Commun. Mass Spectrom. **21**, 3505–3510 (2007)
3. Deng, G., Sanyal, G.: Applications of mass spectrometry in early stages of target based drug discovery. J. Pharm. Biomed. Anal. **40**, 528–538 (2006)
4. Heck, A.J., van den Heuvel, R.H.: Investigation of intact protein complexes by mass spectrometry. Mass Spectrom. Rev. **23**, 368–389 (2004)
5. Pramanik, B.N., Bartner, P.L., Mirza, U.A., Liu, Y.H., Ganguly, A.K.: Electrospray ionization mass spectrometry for the study of non-covalent complexes: an emerging technology. J. Mass Spectrom. **33**, 911–920 (1998)
6. Zhang, J., McCombie, G., Guenat, C., Knochenmuss, R.: FT-ICR mass spectrometry in the drug discovery process. Drug Discov. Today. **10**, 635–642 (2005)

7. Daniel, J.M., Friess, S.D., Rajagopalan, S., Wendt, S., Zenobi, R.: Quantitative determination of noncovalent binding interactions using soft ionization mass spectrometry. Int. J. Mass Spectrom. **216**, 1–27 (2002)

8. Jecklin, M.C., Touboul, D., Bovet, C., Wortmann, A., Zenobi, R.: Which electrospray-based ionization method best reflects protein-ligand interactions found in solution? A comparison of ESI, nanoESI, and ESSI for the determination of dissociation constants with mass spectrometry. J. Am. Soc. Mass Spectrom. **19**, 332–343 (2008)

9. Liu, L., Kitova, E.N., Klassen, J.S.: Quantifying protein-fatty acid interactions using electrospray ionization mass spectrometry. J. Am. Soc. Mass Spectrom. **22**, 310–318 (2011)

10. Peschke, M., Verkerk, U.H., Kebarle, P.: Features of the ESI mechanism that affect the observation of multiply charged noncovalent protein complexes and the determination of the association constant by the titration method. J. Am. Soc. Mass Spectrom. **15**, 1424–1434 (2004)

11. De Vriendt, K., Sandra, K., Desmet, T., Nerinckx, W., Van Beeumen, J., Devreese, B.: Evaluation of automated nano-electrospray mass spectrometry in the determination of non-covalent protein–ligand complexes. Rapid Commun. Mass Spectrom. **18**, 3061–3067 (2004)

12. Robinson, C.V., Chung, E.W., Kragelund, B.B., Knudsen, J., Aplin, R.T., Poulsen, F.M., Dobson, C.M.: Probing the nature of noncovalent interactions by mass spectrometry. A study of protein− CoA ligand binding and assembly. J. Am. Chem. Soc. **118**, 8646–8653 (1996)

13. Wu, Q., Gao, J., Joseph-McCarthy, D., Sigal, G.B., Bruce, J.E., Whitesides, G.M., Smith, R.D.: Carbonic anhydrase-inhibitor binding: from solution to the gas phase. J. Am. Chem. Soc. **119**, 1157–1158 (1997)

14. Chitta, R.K., Rempel, D.L., Gross, M.L.: Determination of affinity constants and response factors of the noncovalent dimer of gramicidin by electrospray ionization mass spectrometry and mathematical modeling. J. Am. Soc. Mass Spectrom. **16**, 1031–1038 (2005)

15. Gabelica, V., Galic, N., Rosu, F., Houssier, C., De Pauw, E.: Influence of response factors on determining equilibrium association constants of noncovalent complexes by electrospray ionization mass spectrometry. J. Mass Spectrom. **38**, 491–501 (2003)

16. Tjernberg, A., Carnö, S., Oliv, F., Benkestock, K., Edlund, P.-O., Griffiths, W.J., Hallén, D.: Determination of dissociation constants for protein− ligand complexes by electrospray ionization mass spectrometry. Anal. Chem. **76**, 4325–4331 (2004)

17. Clark, S.M., Konermann, L.: Determination of ligand− protein dissociation constants by electrospray mass spectrometry-based diffusion measurements. Anal. Chem. **76**, 7077–7083 (2004)

18. Svobodová, J., Mathur, S., Muck, A., Letzel, T., Svatoš, A.: Microchip-ESI-MS determination of dissociation constant of the lysozyme–NAG3 complex. Electrophoresis. **31**, 2680–2685 (2010)

19. Flanigan, P., Levis, R.: Ambient femtosecond laser vaporization and nanosecond laser desorption electrospray ionization mass spectrometry. Annu. Rev. Anal. Chem. **7**, 229–256 (2014)

20. Sampson, J.S., Hawkridge, A.M., Muddiman, D.C.: Generation and detection of multiply-charged peptides and proteins by matrix-assisted laser desorption electrospray ionization (MALDESI) Fourier transform ion cyclotron resonance mass spectrometry. J. Am. Soc. Mass Spectrom. **17**, 1712–1716 (2006)

21. Huang, M.-Z., Hsu, H.-J., Lee, J.-Y., Jeng, J., Shiea, J.: Direct protein detection from biological media through electrospray-assisted laser desorption ionization/mass spectrometry. J. Proteome Res. **5**, 1107–1116 (2006)

22. Brady, J.J., Judge, E.J., Levis, R.J.: Mass spectrometry of intact neutral macromolecules using intense non-resonant femtosecond laser vaporization with electrospray post-ionization. Rapid Commun. Mass Spectrom. **23**, 3151–3157 (2009)

23. Karki, S., Flanigan, P.M., Perez, J.J., Archer, J.J., Levis, R.J.: Increasing protein charge state when using laser electrospray mass spectrometry. J. Am. Soc. Mass Spectrom. **26**, 706–715 (2015)

24. Karki, S., Sistani, H., Archer, J.J., Shi, F., Levis, R.J.: Isolating protein charge state reduction in electrospray droplets using femtosecond laser vaporization. J. Am. Soc. Mass Spectrom. **28**, 470–478 (2017)

25. Shi, F., Flanigan IV, P.M., Archer, J.J., Levis, R.J.: Ambient molecular analysis of biological tissue using low-energy, femtosecond laser vaporization and nanospray postionization mass spectrometry. J. Am. Soc. Mass Spectrom. **27**, 542–551 (2016)

26. Shiea, J., Huang, M.Z., HSu, H.J., Lee, C.Y., Yuan, C.H., Beech, I., Sunner, J.: Electrospray-assisted laser desorption/ionization mass spectrometry for direct ambient analysis of solids. Rapid Commun. Mass Spectrom. **19**, 3701–3704 (2005)

27. Perez, J.J., Flanigan IV, P.M., Karki, S., Levis, R.J.: Laser electrospray mass spectrometry minimizes ion suppression facilitating quantitative mass spectral response for multicomponent mixtures of proteins. Anal. Chem. **85**, 6667–6673 (2013)

28. Nemes, P., Barton, A.A., Li, Y., Vertes, A.: Ambient molecular imaging and depth profiling of live tissue by infrared laser ablation electrospray ionization mass spectrometry. Anal. Chem. **80**, 4575–4582 (2008)

29. Nemes, P., Vertes, A.: Laser ablation electrospray ionization for atmospheric pressure, in vivo, and imaging mass spectrometry. Anal. Chem. **79**, 8098–8106 (2007)

30. Nemes, P., Vertes, A.: Atmospheric-pressure molecular imaging of biological tissues and biofilms by LAESI mass spectrometry. J. Vis. Exp. **43**, e2097 (2010)

31. Robichaud, G., Barry, J.A., Muddiman, D.C.: IR-MALDESI mass spectrometry imaging of biological tissue sections using ice as a matrix. J. Am. Soc. Mass Spectrom. **25**, 319–328 (2014)

32. Shi, F., Archer, J.J., Levis, R.J.: Nonresonant, femtosecond laser vaporization and electrospray post-ionization mass spectrometry as a tool for biological tissue imaging. Methods. **104**, 79–85 (2016)

33. Li, H., Ha, E., Donaldson, R.P., Jeremic, A.M., Vertes, A.: Rapid assessment of human amylin aggregation and its inhibition by copper (II) ions by laser ablation electrospray ionization mass spectrometry with ion mobility separation. Anal. Chem. **87**, 9829–9837 (2015)

34. Lee, E.C., Ha, E., Singh, S., Legesse, L., Ahmad, S., Karnaukhova, E., Donaldson, R.P., Jeremic, A.M.: Copper (II)–human amylin complex protects pancreatic cells from amylin toxicity. Phys. Chem. Chem. Phys. **15**, 12558–12571 (2013)

35. Brady, J.J., Judge, E.J., Levis, R.J.: Nonresonant femtosecond laser vaporization of aqueous protein preserves folded structure. Proc. Natl. Acad. Sci. U. S. A. **108**, 12217–12222 (2011)

36. Akhterov, M.V., Choi, Y., Olsen, T.J., Sims, P.C., Iftikhar, M., Gul, O.T., Corso, B.L., Weiss, G.A., Collins, P.G.: Observing Lysozyme's closing and opening motions by high-resolution single-molecule enzymology. ACS Chem. Biol. **10**, 1495–1501 (2015)

37. Flanigan, P.M., Shi, F., Archer, J.J., Levis, R.J.: Internal energy deposition for low energy, femtosecond laser vaporization and nanospray post-ionization mass spectrometry using thermometer ions. J. Am. Soc. Mass Spectrom. **26**, 716–724 (2015)

38. Flanigan, P.M., Shi, F., Perez, J.J., Karki, S., Pfeiffer, C., Schafmeister, C., Levis, R.J.: Determination of internal energy distributions of laser electrospray mass spectrometry using thermometer ions and other biomolecules. J. Am. Soc. Mass Spectrom. **25**, 1572–1582 (2014)

39. Brady, J.J., Judge, E.J., Levis, R.J.: Analysis of amphiphilic lipids and hydrophobic proteins using nonresonant femtosecond laser vaporization with electrospray post-ionization. J. Am. Soc. Mass Spectrom. **22**, 762–772 (2011)

40. Shi, F., Flanigan IV, P.M., Archer, J.J., Levis, R.J.: Direct analysis of intact biological macromolecules by low-energy, fiber-based femtosecond laser vaporization at 1042 nm wavelength with nanospray postionization mass spectrometry. Anal. Chem. **87**, 3187–3194 (2015)

41. Sistani, H., Karki, S., Archer, J.J., Shi, F., Levis, R.J.: Assessment of reproducibility of laser electrospray mass spectrometry using electrospray deposition of analyte. J. Am. Soc. Mass Spectrom. **28**, 880–886 (2017)

42. Cubrilovic, D., Zenobi, R.: Influence of dimehylsulfoxide on protein–ligand binding affinities. Anal. Chem. **85**, 2724–2730 (2013)

43. Imoto, T., Johnson, L., North, A., Phillips, D., Rupley, J.: 21 vertebrate lysozymes. The enzymes. **7**, 665–868 (1972)

44. Schindler, M., Assaf, Y., Sharon, N., Chipman, D.M.: Mechanism of lysozyme catalysis: role of ground-state strain in subsite D in hen egg-white and human lysozymes. Biochemist. **16**, 423–431 (1977)

45. Yao, Y., Shams-Ud-Doha, K., Daneshfar, R., Kitova, E.N., Klassen, J.S.: Quantifying protein-carbohydrate interactions using liquid sample desorption electrospray ionization mass spectrometry. J. Am. Soc. Mass Spectrom. **26**, 98–106 (2015)

46. Liu, P., Zhang, J., Ferguson, C.N., Chen, H., Loo, J.A.: Measuring protein–ligand interactions using liquid sample desorption electrospray ionization mass spectrometry. Anal. Chem. **85**, 11966–11972 (2013)

47. Judge, E.J., Brady, J.J., Dalton, D., Levis, R.J.: Analysis of pharmaceutical compounds from glass, fabric, steel, and wood surfaces at atmospheric pressure using spatially resolved, nonresonant femtosecond laser vaporization electrospray mass spectrometry. Anal. Chem. **82**, 3231–3238 (2010)